

EXPERIMENTS AT HIGH ELONGATIONS IN DIII-D\*

E.A. LAZARUS,† A.D. TURNBULL, A.G. KELLMAN, J.R. FERRON, F.J. HELTON,  
L.L. Lao, J.A. Leuer, E.J. Strait, and T.S. Taylor

General Atomics  
San Diego, California 92138, U.S.A.

In this paper we discuss the limitation to elongation observed in D-shaped plasmas in the DIII-D tokamak. We find that as the triangularity is increased and  $\ell_i$  is decreased that the  $n = 0$  mode takes on an increasingly non-rigid character. Our analysis shows two aspects of the behavior; first, an increasing variation of the  $m/n = 1/0$  component across flux surfaces and second, an increase in the relative amplitude of a  $m/n = 3/0$  component which couples to the  $m/n = 1/0$  component and further destabilizes the mode.

In previous work<sup>1</sup> we have reported on a study of vertical control and the implementation of those results on DIII-D. In that study we used a single filament, with properties consistent with the radial force balance, to represent the plasma and employed an eigenmode description of the passive shell in order to allow time-ordering of the problem. The most important result of this study was that the active control coil must be positioned in the poloidal plane so as to minimize its interaction with the stabilizing shell currents. As a consequence of plasma toroidicity, these currents flow primarily in the outboard regions of the shell. Thus, control coils on the inboard side of the shell, near the midplane, are required. With such a spatial arrangement we can have radial fields from the active coil penetrating the shell on a time scale faster than the decay of the stabilizing shell currents. In accordance with these model calculations the control system for the DIII-D tokamak has been modified resulting in operation to within a few percent of the ideal MHD limit for axisymmetric stability. In this work we refer to the ideal MHD limit as that of the plasma-shell system. As discussed in Ref. 1, the ideal limit can actually be reduced by a poor choice of the active control coils, however that is not the case for work discussed here.

In Ref. 2 we reported on detailed measurements of the plasma response to that control system and concluded that the model of Ref. 1 is quite accurate and adequate to prescribe the control function. We have also reported in Ref. 2 that the modifications to the control system have enabled us to reach elongation,  $\kappa$ , up to 2.5 transiently and  $\kappa > 2.45$  for more than 0.5 second. Also, behavior characteristic of the destabilisation of the plasma-shell system by use of control coils on the outboard side of the plasma was experimentally observed. With this improved vertical control, operation of double null divertors with elongations of 2.15 have become routine. Behavior at higher elongations is quite sensitive to the plasma shape and the width of the current profile.

The reader may notice small differences in the stability margins quoted here as compared to those in previous work. The primary reason for differences of several percent is that in previous work we had used the contour of the graphite tiles to define the stabilizing shell. In fact, the conducting shell (vacuum vessel wall) is approximately 5 cm. behind the graphite surface and we have now made this correction. Also, we have refined our calculation of  $n_c$ .

EXPERIMENTAL RESULTS

We wish to focus on two particular discharges, #60809 and #63422. The equilibrium parameters for these plasmas are given in Figs. 1 and 2. The equilibria are calculated several milliseconds before the vertical instability which results in disruption. The distinction of interest is that the former has a higher  $\ell_i$  and a lower triangularity,  $\delta$ , than the latter. The motivation for choosing these plasmas is centered about the quantity  $n/n_c$ . The decay index  $n$  is defined as

$$n \equiv - \left. \frac{R}{B_z} \frac{\partial B_z}{\partial R} \right|_{R=R_c, z=z_c}$$

where  $R_c, z_c$  is the centroid of the plasma current. The critical index,  $n_c$ , is

$$n_c \equiv \frac{2M_{vp}^2 R_0}{\mu_0 \Gamma L_v}, \quad \Gamma \equiv \frac{L_{ext}}{\mu_0 R_0} + \frac{\ell_i}{2} + \beta_p + \frac{1}{2}$$

\* Work sponsored by the U.S. Department of Energy under Contract Nos. DE-AC03-89ER51114 and DE-AC05-84OR21400.

† Fusion Energy Division, Oak Ridge National Laboratory, Oak Ridge, Tennessee 37831, U.S.A.

MASTER *de*

## **DISCLAIMER**

This report was prepared as an account of work sponsored by an agency of the United States Government. Neither the United States Government nor any agency thereof, nor any of their employees, makes any warranty, express or implied, or assumes any legal liability or responsibility for the accuracy, completeness, or usefulness of any information, apparatus, product, or process disclosed, or represents that its use would not infringe privately owned rights. Reference herein to any specific commercial product, process, or service by trade name, trademark, manufacturer, or otherwise does not necessarily constitute or imply its endorsement, recommendation, or favoring by the United States Government or any agency thereof. The views and opinions of authors expressed herein do not necessarily state or reflect those of the United States Government or any agency thereof.

$L_{\text{ext}}/(\mu_0 R_0) \approx \ln(8R_c/\bar{a}) - 2$ ,  $\bar{a}$  is the poloidal contour length over  $2\pi$ , and  $\ell_i \equiv [\int_S \alpha^2] \int_V B_p^2 dV / [V \int_S B_p \alpha]^2$ . In Ref. 1  $n/n_c = -1$  was identified as a good approximation for the ideal rigid-body stability limit.

For shot #60809 a value of  $n/n_c = -1.04$  was calculated prior to disruption, whereas for #63422 we could only achieve  $n/n_c = -0.81$ . A multi-filament rigid-body analysis<sup>3</sup> gives similar results, namely values of  $n/n_c$  of 0.91 and 0.73 for #60809 and #63422 respectively. This turns out to be typical of the observed behavior, i.e. as  $\ell_i$  is decreased and  $\delta$  is increased the achievable value of  $n/n_c$  also decreases. This behavior is illustrated in Fig. 3 where we plot the achievable  $n/n_c$  vs.  $\ell_i$ . In column near each data point are  $\kappa$ ,  $\delta$ , and  $Q \equiv [ff]_{\psi=0.95} f_0/R_0/(\kappa q_0)$ , which has been reported<sup>4</sup> as a measure of the departure from rigid-body behavior. In that work Solovev equilibria are used and  $Q$  is purely a shape parameter, whereas here  $Q$  contains effects of the current profile. A correlation in departure from  $n/n_c \sim 1$  is seen with both  $\ell_i$  and with  $Q$ .  $Q$  shows a local sensitivity to the current profile parameterization which is why we chose to plot the data using  $\ell_i$ , a better-known quantity, as the ordinate. In Ref. 4 departure from rigid-body behavior is seen at  $Q < 0$  and  $Q$  is bounded by  $Q > -5$ , thus we consider the agreement to be quite good.

## STABILITY ANALYSIS

In the stability analysis of these plasmas with GATO<sup>5</sup> we use the real wall shape of DIII-D, not a wall conformal to the plasma. This wall has an expansion parameter, which expands the wall in minor radius without changing its shape in the poloidal plane. If, starting with the experimental equilibrium, we find that the expansion parameter must be increased from unity to 1.03 in order to find an instability we shall refer to this as operation at 97% of the ideal limit. For case #60809 the result of this analysis is that we are at 97% of the ideal limit, in good agreement with the rigid-body result of 104%.

For case #63422 the result is 98% of the ideal limit, even though we have only achieved 81% of the rigid-body ( $n/n_c = -1$ ) limit. We will now pursue this discrepancy in a bit more detail. In Fig. 4 we plot the perturbed shape as calculated in GATO and normalized in amplitude so that the perturbed shape of the 95% flux surface just touches the limiting surface of the vessel. The dotted lines are the unperturbed equilibrium. Our control system regulates the vertical position of the current centroid, thus it is of interest to look at this perturbation with the shift in the magnetic axis removed. It can be seen in Fig. 4 that if this axis shift is removed most of the perturbation still remains.

This equilibrium was calculated 2564 ms into the shot. The outer boundary of the plasma at 2566 ms is shown as the broad dashed line in Fig. 4. We see excellent agreement between the calculated and measured deformation of the equilibrium. It is characteristic of vertical disruptions in these D-shaped plasmas that the top of the plasma is moving radially inwards and the bottom radially outwards as the plasma is moving vertically upwards.

As an aid to understanding the perturbation we have spectrally decomposed the results of the GATO calculation. By far the largest component is  $m = 1$ , as shown in Fig. 5. The second largest term is  $m = 3$ , whereas the  $m = 2$  and  $m = 4$  components are negligibly small except at the very edge where the presence of the divertor increases the breadth of the poloidal spectrum. It should be noted that even the  $m = 1$  mode has a distinctly non-rigid character in the outer region of the plasma. By way of comparison, we show in Fig. 6 the spectral decomposition of case #60809. Here all the components other than  $m = 1$  and  $m = 3$  are negligibly small. Because of the higher  $\ell_i$  the  $m = 1$  amplitude peaks in the central region of the plasma. The  $m = 3$  amplitude is about 15% of the  $m = 1$  as opposed to 33% for #63422. These effects combine to account for the much better agreement with the rigid-shift model.

## CONCLUSIONS

We find excellent agreement between the experimentally observed vertical stability limits and ideal MHD stability calculations. Detailed calculation of the perturbed plasma shape done with GATO are in good agreement with experimental observation. The observed behavior is not unexpected. The possibility of an  $m/n = 3/0$  mode was found in the analysis of a square plasma.<sup>6</sup> Departure from a rigid-body stability criterion has been predicted for D-shaped plasmas with high triangularity.<sup>4</sup> Such non-rigid effects have been observed in the PBX tokamak for bean-shaped plasmas.<sup>7</sup>

We find  $n/n_c$  an excellent characterization of the rigid-body stability limit and  $Q$  is in qualitative agreement with the observed departure from rigid-body behavior. As can be seen in Fig. 3, axisymmetric instability is seen over a wide range of elongation. It should be noted that reducing triangularity does not allow higher elongation since the additional quadrupole field required would then simply move the MHD and rigid-body limits closer together. For current profiles typical of DIII-D H-mode plasmas the non-rigid effects have limited our maximum elongation to  $\kappa = 2.5$ .

Over a wide range of plasma conditions we are able to operate to within a few percent of the ideal MHD axisymmetric stability limit. The loss of control is quite abrupt, for instance, we may operate under conditions where  $\kappa = 2.33$  is accomplished without difficulty but  $\kappa = 2.4$  is impossible. Small changes in  $\ell_i$  become critical in such operation.

It remains unclear as to whether this represents the maximum achievable elongation. Of course, some gain is likely from further broadening of the current profile, but these results indicate that further gains will be modest. It is plausible that one could provide further stabilization of the non-rigid component of the motion with other poloidal coils. Because of the shielding effects of the vessel this could only be accomplished with derivative gain. The reference signal would need to be a measure of the difference between the surface motion and that of the axis. Thus the reference signal would be the derivative of a difference signal which involved many magnetic probes. The control function would need to be done without degradation of the axial control. This idea does not violate the above results since the stability calculations only use the passive shell. However, it remains to be seen whether such control is practically realizable. Note that it is only the completeness of the closely-coupled poloidal coil set of DIII-D which allows consideration of such a control scheme.

- 1 Lazarus, E.A., Lister, J.B., Nielson, G.H., Nucl. Fusion 30, (1990) 111.
- 2 Lister, J.B., Lazarus, E.A., Kellman, A.G., et. al., "Experimental Study of the Vertical Stability of High Decay Index Plasmas in the DIII-D Tokamak," General Atomics report GA-A19843, (April 1990), submitted to Nucl. Fusion.
- 3 Leuer, J., Fusion Technol. 15, No. 2 (1989) 489.
- 4 Bernard, L.C., Berger, D., Gruber, R., Troyon, F., Nucl. Fusion 18, (1978) 1331.
- 5 Bernard, L.C., Helton, F.J., Moore, R.W., Comput. Phys. Comm. 24, (1981) 377.
- 6 Rosen, M.D., Phys. Fluids 18, (1975) 482.
- 7 Jardin, S.C., Delucia, M., Okabayashi, M., Pomphrey, N., Reusch, M., et al., Nucl. Fusion 27, (1987) 569.

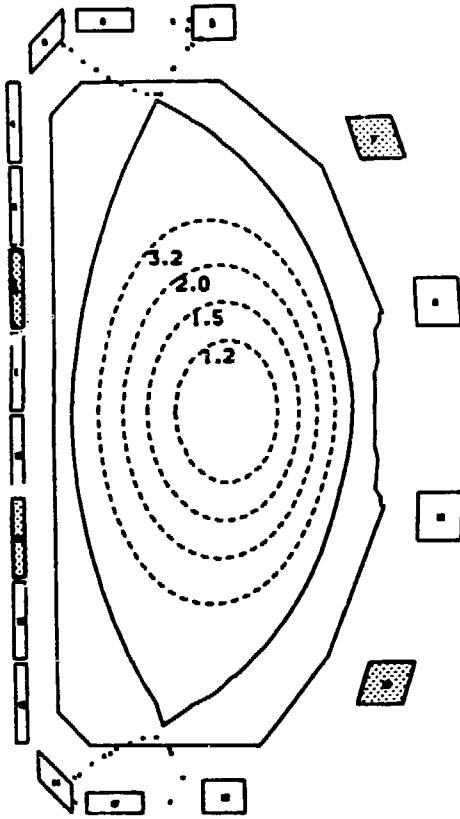


FIG. 1. Shot No. 60809, equilibrium just prior to disruption as calculated from the experimental data. The parameters are  $I_p = 1.0$  MA,  $B_t = 2.0$  T,  $R = 1.69$ ,  $a = 0.59$  m,  $q_{95} = 5.7$ ,  $\beta_p = 0.41$ ,  $\ell_i = 1.48$ ,  $\kappa = 2.17$ , and  $\delta = 0.37$ . The coils used for vertical control are shaded.

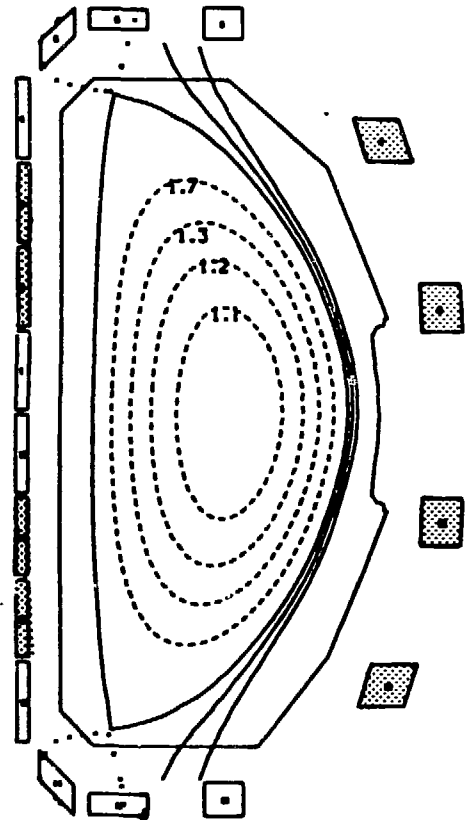


FIG. 2. Shot No. 63422, equilibrium just prior to disruption as calculated from the experimental data. The parameters are  $I_p = 1.1$  MA,  $B_t = 0.8$  T,  $R = 1.69$ ,  $a = 0.54$  m,  $q_{95} = 2.7$ ,  $\beta_p = 0.47$ ,  $\ell_i = 0.92$ ,  $\kappa = 2.41$ , and  $\delta = 0.85$ . The coils used for vertical control are shaded.

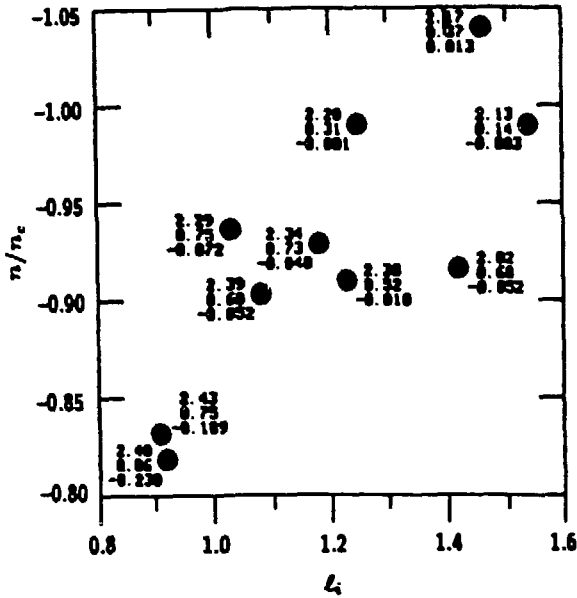


FIG. 3.  $n/n_c$  achieved just before disruption vs.  $l_1$ . Listed at each datum is  $\kappa$ ,  $\delta$ , and  $Q$ .

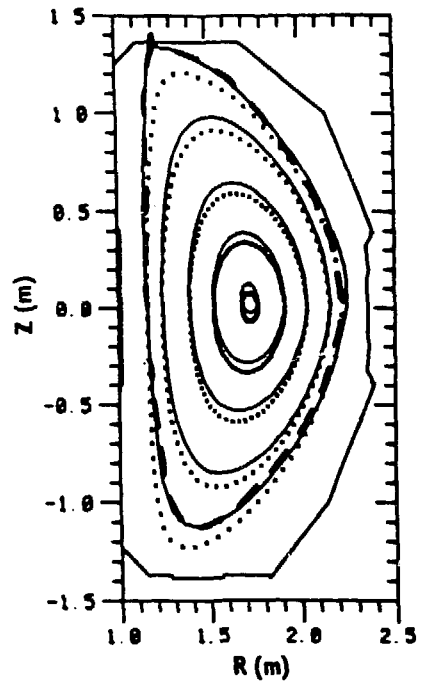


FIG. 4. The perturbation in the equilibrium of case #63422. The dots are the unperturbed equilibrium and the solid lines are the perturbation calculated by GATO with a wall expansion parameter of 1.017. The broad dashed line is the experimentally determined plasma boundary 2 ms later in time.

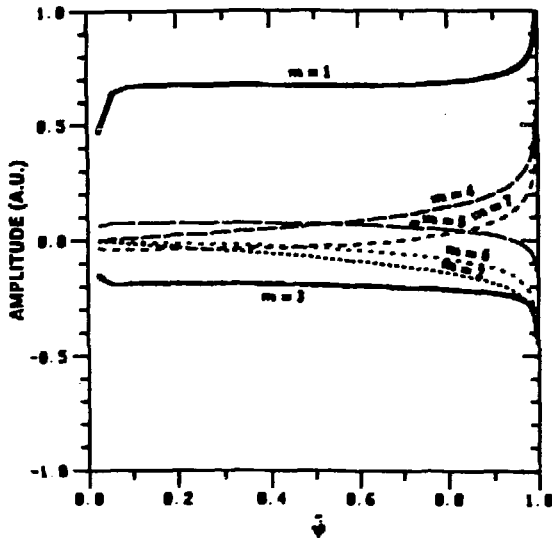


FIG. 5. The poloidal decomposition of the calculated perturbation for case # 63422 normalized to the amplitude of the  $m = 1$  component.

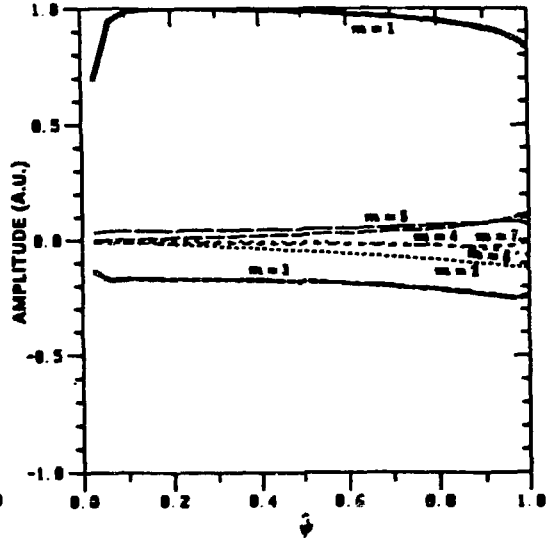


FIG. 6. The poloidal decomposition of the calculated perturbation for case # 60809 normalized to the amplitude of the  $m = 1$  component.